Journal of Intelligent Systems and Internet of Things
Vol. 12, No. 01, PP. 84-96, 2024
DOI: https://doi.org/10.54216/JISIoT.120107

Multimodal Feature Fusion Using Optimal Transfer Learning Approach for Lung Cancer Detection and Classification on CT Images

B. Karthikeyan[1,*], N. Seethalakshmi[2],V. Nandhini[3], D. Vinoth[4], P. Muthusamy[5], Kiran Bellam[6]

[1]Department of Information Technology, Panimalar Engineering College, Chennai, India
[2] C.K. College of Engineering&Technology, Cuddalore-607003, India
[3] Department of Computer Scienec and Engineering, Sona College of Technology, Salem, India;
[4]Department of Computer Science and Engineering, Saveetha School of Engineering, Saveetha Institute of Medical and Technical Sciences, Saveetha University, Chennai, Tamil Nadu, India
[5]Department of Cyber Security, Paavai Engineering College(Autonomous), Namakkal, India
[6]Associate Dean, College of Engineering, Prairie View A & M University, Texas, USA
Emails: karthikeyan.b32@gmail.com; seethan1989@gmail.com; nandinivijaykumar@sonatech.ac.in; vinothd.sse@saveetha.com; muthu.namakkal@gmail.com; kibellam@pvamu.edu
[*]Corresponding Author: karthikeyan.b32@gmail.com

Abstract

Lung cancer detection is the process of detecting the presence of lung tumor or abnormalities in the lungs. Early diagnosis is crucial for increasing the chances of patient survival and successful treatment. When compared to X-rays, Computed Tomography (CT) images are more sensitive and are increasingly being used for the diagnosis and screening of lung tumors. They provide complete cross-sectional images of the lungs and it will even detect small lesions. AI and Machine learning (ML) approaches are most commonly employed to analyse medical images (e.g. CT scans) and detect lung cancer. This algorithm can help radiologists identify patterns indicative or subtle abnormalities of cancer. Medical diagnosis, particularly in complex diseases such as lung cancer, frequently involves ambiguity. The diagnostic system can alleviate ambiguity via cross-verifying findings from various sources by fusing multimodal features. Multimodal feature fusion using deep learning (DL) algorithm is an advanced technology that leverages the abilities of deep neural networks to combine data from three different modalities or sources for better robustness in several applications, namely natural language processing, image, and data analysis, etc. This study introduces a Multimodal Feature Fusion using an Optimal Transfer Learning Method for Lung Cancer Detection and Classification (MFFOTL-LCDC) methodology on CT images. The chief objective of the MFFOTL-LCDC methodology is to exploit the feature fusion process for the identification and classification of lung tumor. To attain this, the MFFOTL-LCDC model undergoes a multimodal feature fusion approach to derive feature vectors using 3 DL approaches such as SqueezeNet, CapsNet, and Inception v3 models. Besides, the MFFOTL-LCDC technique applies the remora optimization algorithm (ROA) for the hyperparameter choice of 3 DL models. For lung cancer recognition, the MFFOTL-LCDC algorithm exploits the deep extreme learning machine (DELM) algorithm. A series of simulations were conducted to ensure the greater lung cancer recognition outcomes of the MFFOTL-LCDC methodology. The extensive outcomes determine the improved results of the MFFOTL-LCDC technique over recent DL approaches.

Received: August 26, 2023 Revised: November 19, 2023 Accepted: February 25, 2024

Keywords: Lung cancer; Multimodality; Feature fusion; Deep learning; CT images; Computer-aided diagnosis

1. Introduction

Lung cancer is one of the widespread life-threatening diseases that has been evaluated 422 survive worldwide daily. Persons above the age of 50 commonly develop cancer therefore, many lung cancer cases are rising day-by-day [1]. It is regarded as a major cause of fatality due to lung cancer being challenging to diagnose compared to other diseases. The main cause of failure is the smaller size of the lesion which can be described as a nodule [2]. Cancer cell size is small in an early phase however; it increases and develops malignant after a specified time. Thus, controlling the cancer at an earlier phase is significant. When cancer is diagnosed earlier, the survival rate could be enhanced. Currently, computer vision (CV) research workers are designing high-technology networks, which automatically diagnose and recognize normal and cancerous regions [3]. Initially, the radiologists categorize a possible node as malignant or benign by the CT image examination that has a more difficult and time consuming method. Besides, this classification must be extremely reliant on the capability of the radiologists. Hence, to address these problems, computer aided diagnostic (CAD) models was employed [4].

The diagnostic and predictive techniques are improved quickly because of the developments in the medical field [5]. While operative feature extraction techniques are needed to attain better performance, Deep learning (DL) algorithms are popularly utilized in the medical field for automatic deep feature extraction. Machine learning (ML) is a domain of artificial intelligence (AI) that must be developed from the analysis of pattern recognition and cognitive learning principles. It is considered to make techniques and models, which can be capable of learning and modifying from wide-ranging databases [6]. By leveraging this data, ML techniques could be selected and predicted depending on previous patterns and knowledge. ML methods have been developed for analyzing and extracting useful data from massive databases. This can be recognized in correlations, patterns, and trends, which cannot be obvious to human beings [7]. DL has a progressive model ML that is excellent in tasks namely voice recognition, feature extraction, object detection, and other fields, which include intricate data processing. It employs deep neural network (DNN) with numerous layers for extracting and learning difficult patterns from datasets. DL has established excellent abilities in different domains and is evident to attain high levels of effectiveness, sometimes exceeding human performance [8]. Transfer learning (TL) is a method in ML and DL models that includes employing previous knowledge achieved from one task to enhance the effectiveness of other relevant tasks. TL is especially valuable if it is confined to labelled data accessible for decided tasks [9]. It is implemented in two methods namely as a baseline technique, employed for training the image database and estimating performance; and as a feature extractor, when features could be extracted from image databases and utilized with both ML and DL techniques to evaluate the performances. Alternatively, Ensemble learning comprises incorporating many decisively established learning methods to overcome issues like classification [10]. It has an ML algorithm that goals to improve the accuracy of prediction by combining several techniques. Also, it can be a leading field of research to enhance base classification methods.

This article introduces a Multimodal Feature Fusion using the Optimal Transfer Learning Method for Lung Cancer Detection and Classification (MFFOTL-LCDC) system on CT images. The MFFOTL-LCDC technique undergoes a multimodal feature fusion approach to derive feature vectors using 3 DL approaches such as SqueezeNet, CapsNet, and Inception v3 models. Besides, the MFFOTL-LCDC technique applies the remora optimization algorithm (ROA) of 3 DL models. For lung cancer recognition, the MFFOTL-LCDC methodology exploits the deep extreme learning machine (DELM) model. To safeguard the enhanced lung cancer recognition results of the MFFOTL-LCDC methodology, a sequence of simulations can performed.

2. Related Works

Raza et al. [11] recognized a new TL-based forecaster named, Lung-EffNet for classifying lung tumors. Lung-EffNet has made depends on the framework of EfficientNet. Lung-EffNet was estimated with the help of 5 variants of EfficientNet like B0–B4. Chenyang and Chan [12] introduced a combined lung nodule identification and classification network. Both the nodule identification and classification sub-networks of this designed combined network modify a 3D encoder-decoder model for effectively analyzing the 3D data. Furthermore, the classification sub-network employs feature extraction from the identification sub-network and multi-scale nodule-related features for improving the classification effectiveness. In [13], the authors introduced a cat swarm optimizer based CAD architecture for lung cancer classification (CSO-CADLCC) method. This technique employs a Gabor filtering-related noise removal approach. This framework was developed by the CSO technique with the WELM algorithm that was employed for classifying lung nodules. Eventually, the CSO method was employed for hyperparameter tuning.

Vishwa Kiran et al. [14] designed an automated ML method with data science assisted lung cancer diagnosis and classification (MLDS-LCDC) technique. Further, it is provided in the normalized cuts (Ncuts) algorithm. Additionally, the oriented FAST and rotated BRIEF (ORB) approach was employed for extracting features. Lastly, the sunflower optimizer based wavelet NN (SFO-WNN) technique was exploited for the classification. Shankara and

Hariprasad [15] implemented image processing methods and an ANN for making an automated technique. In the primary stage, image noise reduction, the histogram for image improvement, Thresholding for morphological processes (dilation), GLCM, object edge identification, and image segmentation were employed for extracting features. In the secondary stage, the ANN is built by applying an ML approach. In [16,] an innovative DL technique was presented. Firstly, Step Deviation Mean Multi-level Thresholding (SDMMT) and event-net classifier are exploited for classification and pre-processing.

Nawreen et al. [17] introduced a new technique of lung tumor identification by utilizing image processing. Further, thresholding and edge identification for segmenting ROI of the lung cancer was implemented. Lastly, numerous geometrical extracted features ROI and classifying into severity grade with the help of the SVM method were estimated. In [18], lung cancer classification and identification with CT images dependent upon hybrid DL (LNDC-HDL) methods are developed. Primarily, the authors presented a chaotic bird swarm optimizer (CBSO) technique for the segmentation through statistical data. Secondarily, the authors described an improved Fish Bee (IFB) method for feature selection (FS) and extraction. Lastly, the authors proposed a HDE-NN to forecast and identify cancer.

3. The Proposed Model

In this article, we have projected the MFFOTL-LCDC methodology for lung cancer identification and recognition on CT scans. The MFFOTL-LCDC model main goal is to exploit the procedure of feature fusion for detection of lung tumors. In order to achieve this, the MFFOTL-LCDC approach undergoes numerous processes such as multimodal feature fusion, ROA based hyperparameter tuning, and DELM based detection. Fig. 1 denotes the summary of the MFFOTL-LCDC technique.

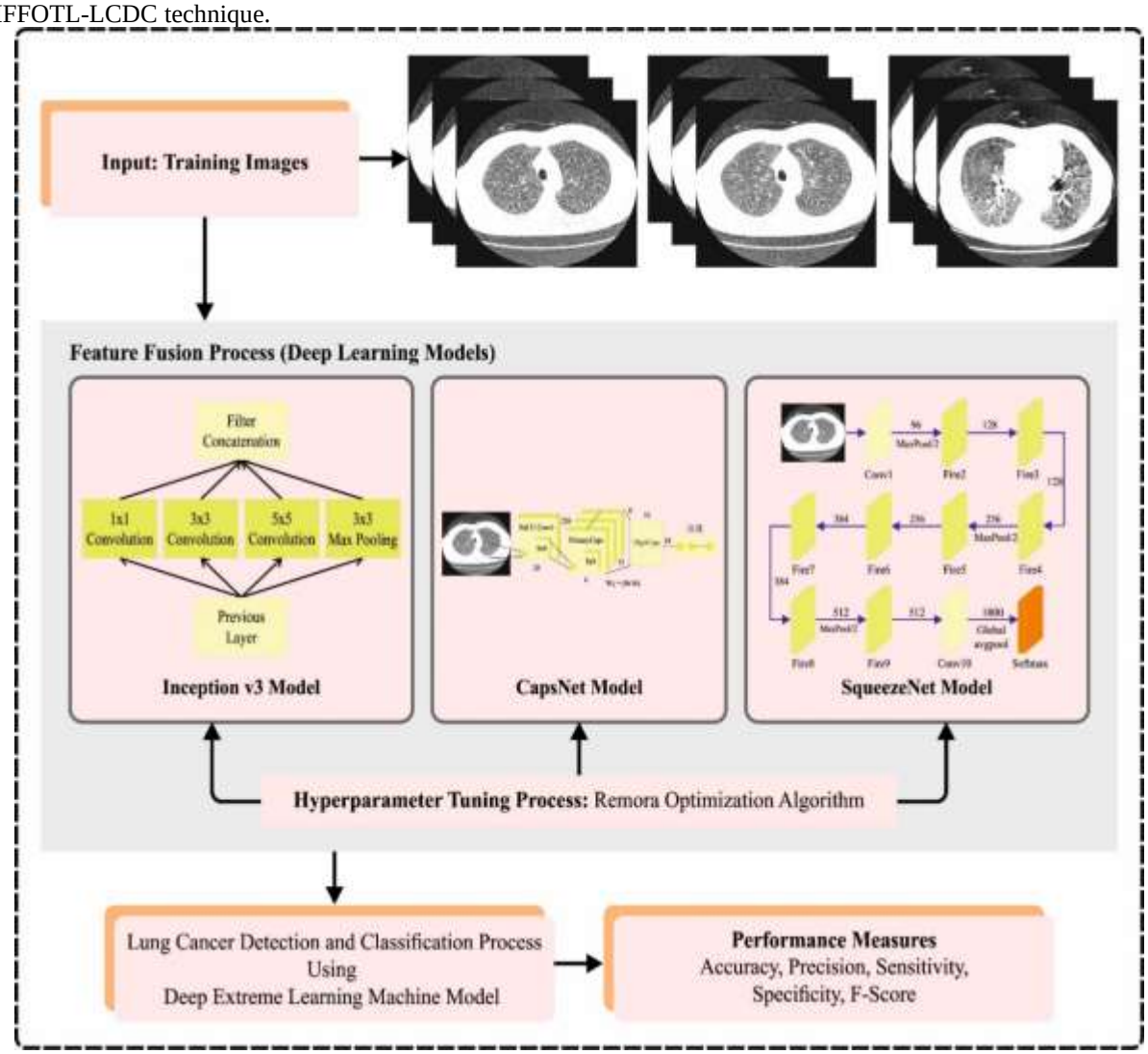

Figure 1: Workflow of MFFOTL-LCDC algorithm

A. Multimodal Feature Fusion Process

In this work, a multi-modal feature fusion technique is difficult to stem feature vectors by utilizing three DL approaches namely CapsNet, SqueezeNet, and Inceptionv3 models. The entropy based feature fusion (EFF) technique is mainly utilized for the purpose of feature extractor. In the method of image processing, the EFF model is employed and ML model integrates numerous feature vectors into a single vector with a highest content of data. The foremost target is to increase the exactness and sturdiness of the ML system by eliminating the appropriate info from diverse features and integrating them into a solitary feature vectors. The following steps include the typical process of entropy-based feature fusion:

- Feature Extractor: Different features are removed from the input data via dissimilar algorithms.
- Feature Normalization: At the time of fusion process, the feature extractor was regularized to ensure that each feature had a comparable weight.
- Feature Weighting: Based on the entropy values, all the features can assigned a weight evaluated by the amount of information added to the feature. Features with highest entropy values give high weights at the time of fusion procedure.
- Feature Fusion: The weighted features are combined into a single feature vector employing a weighted sum.
- In numerous applications such as image processing, speech recognition, and object recognition, the entropy-based feature fusion method has been used. The method increases the accuracy and robustness of the ML method by combining multiple features into a single feature vector, making them better in practical application.

1. CapsNet Model

The simple module in the CapsNet is a capsule which includes a group of neurons that shows the instantiation parameter of specific types of entities namely objects or object parts [19], A high-level capsule signifies intricate entities with a high degree of liberty. The first capsule renders the lowest level of multiple-dimension units and categorized are longer instantiation vector for input that are the highest level representatives of object portion. This distance signifies the possibility and a long length represents the possible solution for the classification task. The lowest level capsule has been reallocated to the highest level capsule which is classified by various types of computation called dynamic routing. The routing algorithm assigns a capsule depend on vector which has a large scalar product as an iterative routing contract method on the supervised data, In addition, it makes sure that the capsule categorized may forecast input classes through the length, and analogous representation may attain essential data from the features for modernization. But new routing need a unsupervised learning. The system exploits the regularized model for boosting the accuracy and mitigates over-fitting on some major classification databases. During the training, a mask matrix was applied to cover each with zeros and newly categorized capsule was smoothened to the vector as a representation of CapsNet. The reconstruction system recreates the image from the representation but maintains vital information.

2. SqueezeNet Model

The SqueezeNet model is the most effective and preferable technique for several applications of CV [20]. This is due to the many hidden layers (HL) used to build the SqueezeNet model, and in this method, the hyperparameter settings are customized. Due to these features, the feature extraction network learned the internal representation of signal dimensional for the feature learning algorithm and used the standardized procedure on 1D signals from the condition e.g., time sequence. SqueezeNet has convolution and pooling layers that have received signal as an input. With the convolution kernels, the signal feature mapping is obtained by the applications of convolution operation to input signal in the convolution function.

In the mapping feature of the convolution layer, the local features are abstracted by the pooling layer through sampling operation for reducing the dimensionality of variables and neurons. A deep architecture can be developed by combining the convolution layer with pooling layers and abstracting the action feature information in the new action data. Consequently, it provides different feature maps with action features. The convolution layer combines the signal with the 2D convolution kernels from the various adjacent frames. The 3 convolution layers' related convolution kernel number includes 72, 18, and 36.

$$f(x) = \max(0, x) = \begin{cases} 0, & x < 0, \\ x, & x \geq 0. \end{cases} \tag{1}$$

Further, we have:

$$f'(x) = \begin{cases} 0, & x < 0, \\ 1, & x \geq 0. \end{cases} \tag{2}$$

In this work, convolution sizes of 2×36, 2×8, and 2×18 kernels were used with the step one size. Convolution processing seems to be impossible while the filter could not deal with the information in a specific direction. The

declining signal data may be avoided by presenting the padding variables, setting it to "SAME", and including 0 to the edge of an input signal. A nonlinear activation operation is used after the convolution function to the output in the convolution layer and generates an output of the convolution layer. During the feature extraction, the positive data value remained the same, and the negative data value was converted into 0 using the ReLu function.

3. Inceptionv3 Model

The Inception module of CNN is considered to be a sequence of NNs that must be excluded from the records of CNNs [21]. Several NN carry out only the network expansion process by enhancing the convolution function to achieve the optimum function. It has changed the predetermined principles. The Inception model derived from the Inception NN exploits different filter kernels and high pooling for limiting the data size. There is a tremendous advantage of getting features with limited variables and meaningfully diminished processes. Inception_v3 applied the asymmetric module for degrading large-scale convolutional kernels into the small-scale convolutional kernel that minimizes the 3x3 convolutional kernels into 2 convolutional sizes of $1x3$, and $3x1$, as well as limits the network variable while provisioning performance of the network. The depth of NN can be deepened and the nonlinearity of the system was increased during the application of asymmetric decomposition. Usually, the CNN pooling operation is used to lessen the mesh size of mapping features. Before applying max or average pooling, the activation dimension of network activation must be expanded to eliminate the problems.

B. Hyperparameter Tuning using ROA

To choose the hyperparameters associated to the DL models, the ROA can employed. ROA is a nature-inspired, bionic metaheuristic that simulates the attaching process of remora to a host of dissimilar body sizes thereby completing the foraging task [22]. Compared with other metaheuristic approaches, ROA is mathematically simulated for kinetic behaviour and kinetic patterns. Comparisons and statistical analysis indicate that ROA shows strong competitiveness and higher application prospects than other advanced heuristics. Thus, it is considered to be applied to the multi-objective optimization of power system tides to attain the best tide outcomes.

Remora is a carnivorous marine fish, that frequently uses a suction cup to attach to the bottom of the boat or other large fish to seek food and swim far. While there is not sufficient food around to survive, Remora tries to find a nearby host to attach to. Based on the elite concept of SOA, the carp position updating formula is given below:

$$X(k+1) = X_{Best}(k) - \left(rand * \left(\frac{X_{Best}(k) + X_{rmd}(k)}{2} \right) - X_{rand}(k) \right) \quad (3)$$

In Eq. (3), k refers to the number of existing iterations, X shows the individual after location update, X_{rand} indicates the randomly selected individuals, and X_{Best} shows the individual population before updating the position. The equation mainly exploits the optimum individual guidance mechanism while adding a random selection rule to make sure the search space.

Simultaneously, Remora considers whether it is essential to change the host while adsorbing on the present host. Thus, the fish need to continuously make smaller movements around the host, which is the adaptive behaviour of fish to its safety, and avoid the host from being attacked. Such behaviours are formulated by:

$$X_{fit}(k+1) = X(k) + \left(X(k) - X_{pre}(k) \right) * randn \quad (4)$$

In Eq. (4), X_{pre} denotes the location of the prior generation. X_{fit} indicates the fitness values of the existing location. When the remora finds the best boat bottom or other large fish, they attach themselves to the body of the host for longer voyages and pursue food to save energy while being protected from enemy attack. The location updating equation is given below:

$$X(k+1) = Dist * e^{\alpha} * \cos(2\pi\alpha) + X(k) \quad (5)$$

$$\alpha = rand * (a-1) + 1 \quad (6)$$

$$a = -\binom{1+\frac{k}{K}} \quad (7)$$

$$Dist = |X_{Best}(k) - X(k)| \quad (8)$$

Now D_{ist} shows the distance among the prey and remora, k denotes the existing iteration counts; K shows the overall amount of iterations set; α refers to the random value within [-1, 1], a is a random integer within [-2,-1].

Once the remora get food-rich water, they detach from the present host and begin the procedure of localized search for food.

$$X(k+1) = X(k) + A \quad (9)$$

$$A = B * \left(X(k) - C * X_{Best}(k) \right) \quad (10)$$

$$B = 2V * rand - V \quad (11)$$

$$V = 2\left(1 - \frac{k}{K}\right) \tag{12}$$

Where A refers to the moving step, and its value is related to the existing remora fish and dimension. As well, the Parameter C was also used for mapping the location of the remora to control the host-to-remora stature ratio. Assume that the host volume is 1, the remora is a small fraction of the host volume, and consider C as a random value within [0,0.3].

The fitness optimal is a foremost reason in the ROA approach. An encrypted result is employed to evaluate the outstanding performance of candidate outcomes. Here, the values of accuracy are the most essential condition employed to design an FF.

$$Fitness = \max(P) \tag{13}$$

$$P = \frac{TP}{TP + FP} \tag{14}$$

Whereas FP and TP represents false and true positive values.

C. Image Classification utilizing DELM Model

For lung cancer detection, MFFOTL-LCDC algorithm utilizes the DELM model. DELM is a deep network constructed from multiple stacked ELM-AE [23]. The ELM exhibits powerful generalization abilities to handle non-linear problems, efficiently extracting data from information through the hierarchical learning model that progresses from easy to complicated features. ELM forms ELM-AE when combined with AE which estimates the new input matrix by minimalizing reconstructed errors. In comparison with classical DNN, DELM is used to maintain remarkable generalization performance while providing fast training speed. Fig. 2 depicts the infrastructure of ELM.

DELM is used to adapt the ELM-AE encoding architecture for obtaining a flattened representation of data layer-wise, which maps the information x to H HL. The output weight β of ELM-AE is accountable for learning transformation in feature space to the input dataset.

$$H = f(W \cdot x + b) \tag{15}$$

$$\beta = \left(\frac{I}{C} + H^T H\right)^{-1} H^T X \tag{16}$$

From the expression, W refers to the input to HL input weights, f exploits the function of sigmoid activation, b shows the bias, I denotes the identity matrix, and C represents the regularized co-efficient. For the Hi of i^{th} layer ELM-AE outcome, it can be shown as follows:

$$H_i = g(H_{i-1} \cdot \beta_i) \tag{17}$$

In contrast with single-layer ELM, DELM has the most powerful ability for representation learning. DELM exploits a layer-wise learning algorithm, gradually extracting data from easy to difficult features. During the learning process, this hierarchical learning algorithm enables reiteratively enhancing the feature representation thus improving its generalization capability.

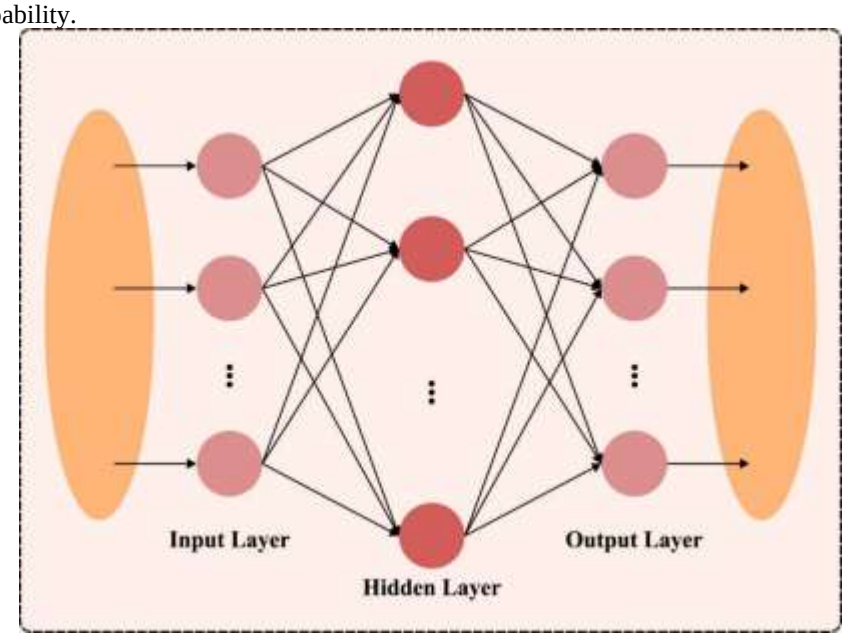

Figure 2: ELM architecture

4. Results and Discussion

The lung cancer detection results of the MFFOTL-LCDC method are tested by employing the dataset [24], containing 100 instances with 3 classes as signified in Table 1.

Table 1 Dataset details

Classes	No. of Instances
Normal	35
Benign	32
Malignant	33
Total Instances	100

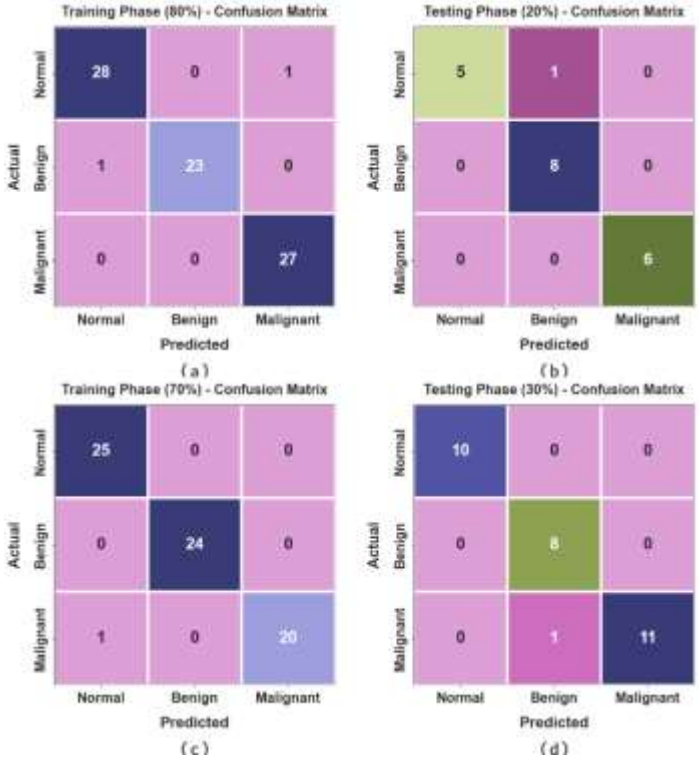

Figure 3: Confusion matrices of (a-b) 80:20 of TRAP/TESP and (c-d) 70:30 of TRAP / TESP

Fig. 3 represents the confusion matrices produced by the MFFOTL-LCDC model at 80:20 and 70:30 of the TRAP/TESP. The outcomes referred to the effective recognition and classification of 3 class labels. In Table 2 and Fig. 4, the lung cancer detection results of the MFFOTL-LCDC technique is given under 80:20 of the TRAP/TESP. These experimental values indicate that the MFFOTL-LCDC technique correctly categorized the normal, benign, and malignant instances.

Table 2: Lung cancer detection analysis of MFFOTL-LCDC model at 80:20 of TRAP/TESP

Classes	$Accu_y$	$Prec_n$	$Sens_y$	$Spec_y$	F_{Score}
TRAP (80%)					
Normal	97.50	96.55	96.55	98.04	96.55
Benign	98.75	100.00	95.83	100.00	97.87
Malignant	98.75	96.43	100.00	98.11	98.18
Average	98.33	97.66	97.46	98.72	97.54
TESP (20%)					
Normal	95.00	100.00	83.33	100.00	90.91
Benign	95.00	88.89	100.00	91.67	94.12
Malignant	100.00	100.00	100.00	100.00	100.00
Average	96.67	96.30	94.44	97.22	95.01

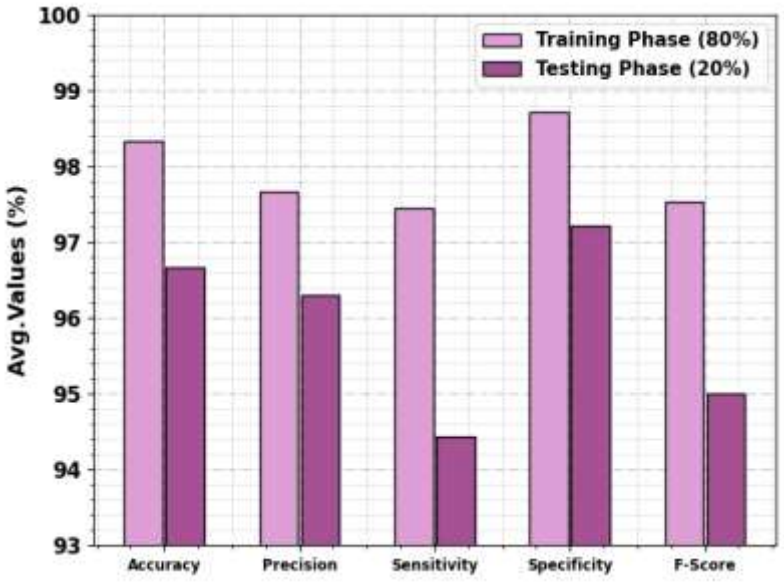

Figure 4: Average of MFFOTL-LCDC systems at 80:20 of TRAP /TESP

With 80% of the TRAP, the MFFOTL-LCDC technique gains average $accu_y$, $prec_n$, $sens_y$, $spec_y$, and F_{score} of 98.33%, 97.66%, 97.46%, 98.72%, and 97.54% respectively. Besides, with 20% of the TESP, the MFFOTL-LCDC methodology achieves average $accu_y$, $prec_n$, $sens_y$, $spec_y$, and F_{score} of 96.67%, 96.30%, 94.44%, 97.22%, and 95.01%, consistently.

In Table 3 and Fig. 5, the lung cancer recognition result of MFFOTL-LCDC method is given under 70:30 of the TRAP/TESP. These simulation values implied that the MFFOTL-LCDC algorithm properly classified the normal, benign, and malignant samples. With 70% of the TRAP, the MFFOTL-LCDC algorithm attains average $accu_y$, $prec_n$, $sens_y$, $spec_y$, and F_{score} of 99.05%, 98.72%, 98.41%, 99.26%, and 98.53% respectively. Also, with 30% of the TESP, the MFFOTL-LCDC methodology achieves average $accu_y$, $prec_n$, $sens_y$, $spec_y$, and F_{score} of 97.78%, 96.30%, 97.22%, 98.48%, and 96.59% respectively.

Table 3: Lung cancer detection outcome of MFFOTL-LCDC algorithm at 80:20 of TRAP/TESP

Classes	$Accu_y$	$Prec_n$	$Sens_y$	$Spec_y$	F_{Score}
TRAP (70%)					
Normal	98.57	96.15	100.00	97.78	98.04
Benign	100.00	100.00	100.00	100.00	100.00
Malignant	98.57	100.00	95.24	100.00	97.56
Average	99.05	98.72	98.41	99.26	98.53
TESP (30%)					
Normal	100.00	100.00	100.00	100.00	100.00
Benign	96.67	88.89	100.00	95.45	94.12
Malignant	96.67	100.00	91.67	100.00	95.65
Average	97.78	96.30	97.22	98.48	96.59

To estimate the performance of the MFFOTL-LCDC approach at 70:30 of the TRAP/TESP, TRA and TES $accu_y$ curves are definite, as represented in Fig. 6. The TRA and TES $accu_y$ curves signify the outcome of the MFFOTL-LCDC model under many epochs. The figure offers significant details assuming the learning task and generalized capabilities of the MFFOTL-LCDC method. With a superior epoch count, it can be clear that the TRA and TES $accu_y$ curves achieve higher. It can be experimental that the MFFOTL-LCDC approach extents better testing accuracy which can recognize the patterns in the TRA and TES data.

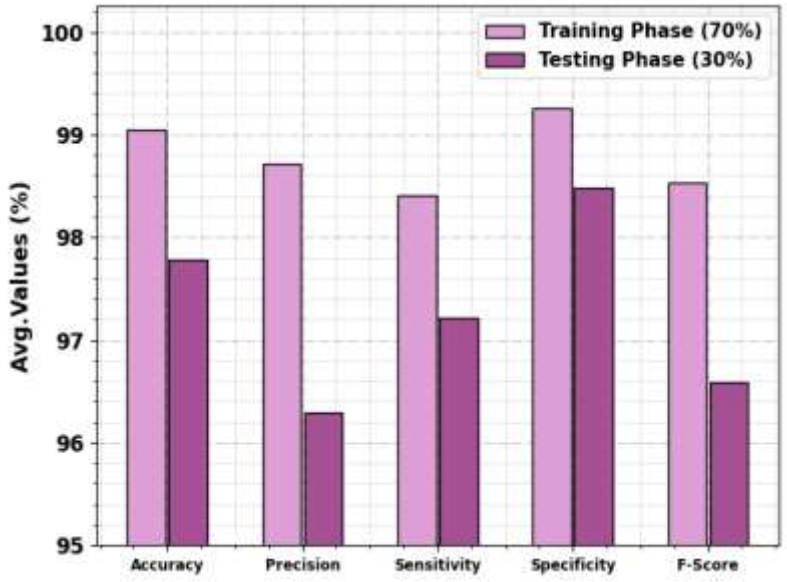

Figure 5: Average of MFFOTL-LCDC algorithm at 70:30 of TRAP/TESP

Figure 6: $Accu_y$ curve of MFFOTL-LCDC algorithm at 70:30 of TRAP/TESP

Fig. 7 shows the complete TRA and TES loss values of the MFFOTL-LCDC algorithm at 70:30 of the TRAP/TESP over epochs. The TRA loss reveals the technique loss is lesser over epochs. Chiefly, the loss values are condensed as the model adapts the load to lessen the forecast fault on the TRA and TES data. The loss curves establish the amount to which the model fits the training data. It is perceived that the TRA and TES loss is steadily lesser and defined that the MFFOTL-LCDC methodology efficiently learns the designs displayed in the TRA and TES data. It was also detected that the MFFOTL-LCDC method adjusted the parameters to reduce the difference among the prediction and original training labels.

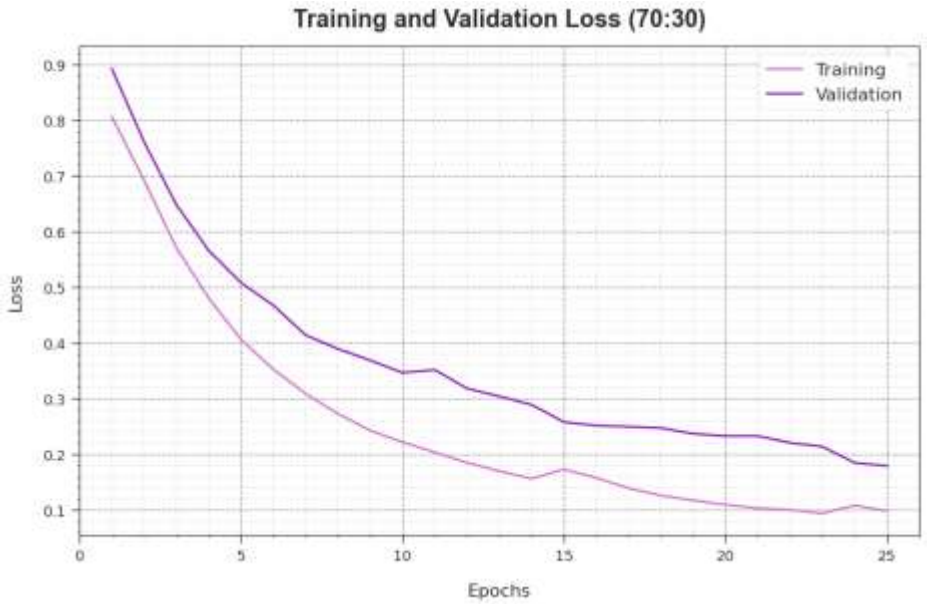

Figure 7: Loss curve of MFFOTL-LCDC algorithm at 70:30 of TRAP/TESP

The precision recall curve of the MFFOTL-LCDC technique at 70:30 of the TRAP/TESP is depicted by plotting accuracy against recall as definite in Fig. 8. The results authorize that the MFFOTL-LCDC model attains highest precision-recall values below all class labels. The figure illustrates that the model learns to distinguish various classes. The MFFOTL-LCDC technique realizes higher outcomes in the recognition of positive examples with least false positives.

The ROC curves presented by the MFFOTL-LCDC methodology at 70:30 of the TRAP/TESP are verified in Fig. 9, which has the ability to distinguish the class labels. The figure points out valued insights into the trade off among the TPR and FPR rates over separate classification thresholds and variable epochs counts. It presents the precise predictive result of the MFFOTL-LCDC technique on the categorization of several class labels.

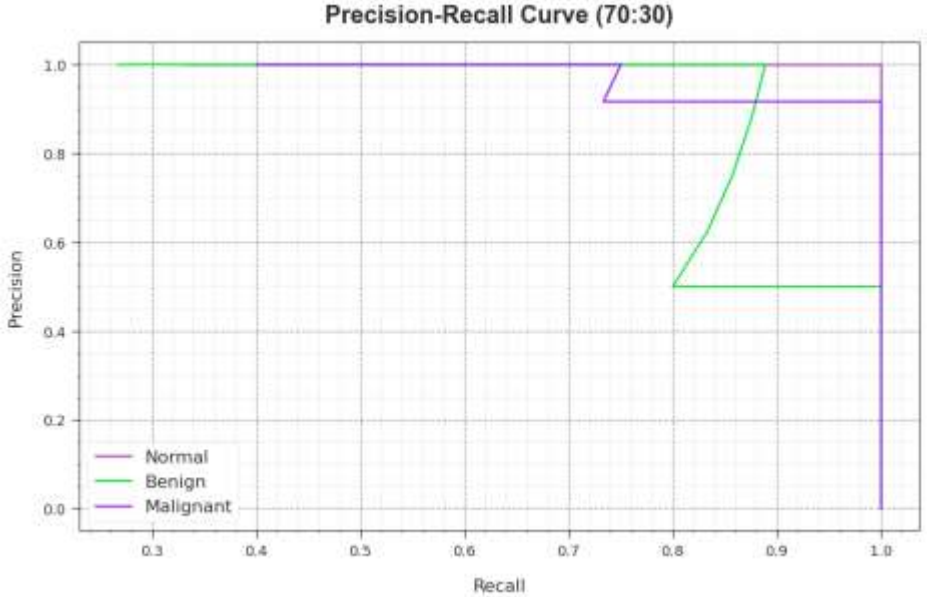

Figure 8: PR curve of MFFOTL-LCDC algorithm at 70:30 of TRAP/TESP

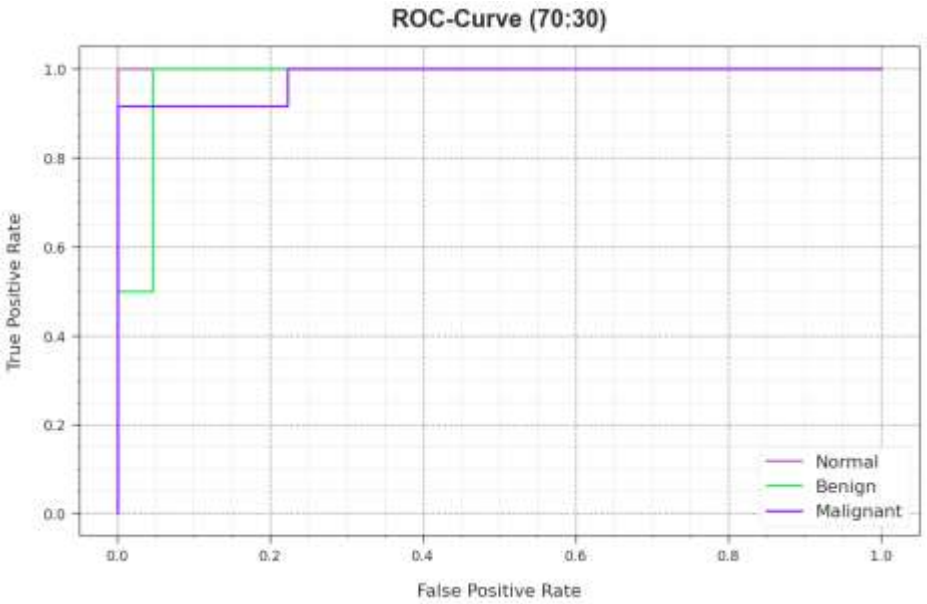

Figure 9: ROC curve of MFFOTL-LCDC algorithm at 70:30 of TRAP/TESP

The comparison research of the MFFOTL-LCDC model is delivered in Table 4 and Fig. 10 [25-27]. The simulation values signify that the MFFOTL-LCDC technique reaches improved performance. Based on $accu_y$, the MFFOTL-LCDC technique gains an increased value of 99.05% but the ODNN, KNN, DNN, YOLODLN, DBNLND, and AGFLCCDGM techniques obtain decreased $accu_y$ values of 92.29%, 96.68%, 95.62%, 94.92%, 95.18%, and 98.94% similarly.

Table 4: Comparative outcome of MFFOTL-LCDC system with existing algorithms

Methods	Accuracy	Precision	Sensitivity	Specificity
ODNN	92.29	91.45	88.72	88.70
KNN	96.68	97.19	86.61	92.26
DNN	95.62	97.13	93.03	89.58
YOLODLN	94.92	96.65	94.85	95.28
DBNLND	95.18	98.10	93.67	90.35
AGFLCCDGM	98.94	97.06	97.31	99.07
MFFOTL-LCDC	99.05	98.72	98.41	99.26

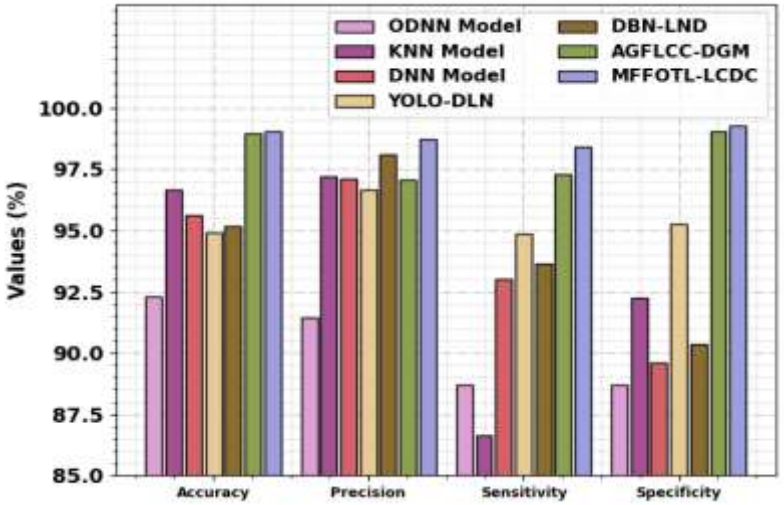

Figure 10: Comparative outcome of MFFOTL-LCDC algorithm with existing algorithms

Followed by, based on $prec_n$, the MFFOTL-LCDC approach reaches a higher value of 98.72% whereas the ODNN, KNN, DNN, YOLODLN, DBNLND, and AGFLCCDGM algorithms reach lesser $prec_n$ values of 91.45%, 97.19%, 97.13%, 96.65%, 98.10%, and 97.06% correspondingly. Finally, based on $sens_y$, the MFFOTL-LCDC methodology attains a higher value of 98.41% but the ODNN, KNN, DNN, YOLODLN, DBNLND, and AGFLCCDGM methodologies reach minimal $sens_y$ values of 88.72%, 86.61%, 93.03%, 94.85%, 93.67%, and 97.31% correspondingly. These results pointed out the enhanced lung cancer detection outcome of the MFFOTL-LCDC approach.

5. Conclusion

In this paper, we have been proposed the MFFOTL-LCDC methodology for lung cancer detection and identification on CT scans. The foremost main of the MFFOTL-LCDC system is to exploit the feature fusion process for the classification and identification of lung tumours. To achieve this, the MFFOTL-LCDC technique undergoes several procedures such as multimodal feature fusion, ROA-based hyperparameter tuning, and DELM-based classification. Here, a multimodal feature fusion approach is involved to derive feature vectors using 3 DL approaches such as SqueezeNet, CapsNet, and Inception v3 models. Besides, the MFFOTL-LCDC technique exploited the ROA for the hyperparameter choice of the 3 DL models. For lung cancer recognition, the MFFOTL-LCDC methodology exploits the DELM model. A series of simulations were conducted to ensure the greater lung cancer detection outcomes of the MFFOTL-LCDC algorithm. The extensive results validate the upgraded outcomes of the MFFOTL-LCDC technique over recent DL methodologies.

Funding: "This research received no external funding"

Conflicts of Interest: "The authors declare no conflict of interest."

References

[1] Tyagi, S. and Talbar, S.N., 2023. LCSCNet: A multi-level approach for lung cancer stage classification using 3D dense convolutional neural networks with concurrent squeeze-and-excitation module. Biomedical Signal Processing and Control, 80, p.104391.

[2] Agarwal, A., Patni, K. and Rajeswari, D., 2021, July. Lung cancer detection and classification based on alexnet CNN. In 2021 6th International Conference on Communication and Electronics Systems (ICCES) (pp. 1390-1397). IEEE.

[3] Sourlos, N., Wang, J., Nagaraj, Y., van Ooijen, P. and Vliegenthart, R., 2022. Possible Bias in Supervised Deep Learning Algorithms for CT Lung Nodule Detection and Classification. Cancers, 14(16), p.3867.

[4] Riquelme, D. and Akhloufi, M.A., 2020. Deep learning for lung cancer nodules detection and classification in CT scans. Ai, 1(1), pp.28-67.

[5] Saturi, S. and Sandhya, B., 2022, October. Cancer Detection and Classification Using 3D-Convolutional Neural Networks. In 2022 IEEE 2nd Mysore Sub Section International Conference (MysuruCon) (pp. 1-7). IEEE.

[6] Zhao, H., Su, Y., Lyu, Z., Tian, L., Xu, P., Lin, L., Han, W. and Fu, P., 2023. Non-invasively Discriminating the Pathological Subtypes of Non-small Cell Lung Cancer with Pretreatment 18F-FDG PET/CT Using Deep Learning. Academic Radiology.

[7] Sajja, T., Devarapalli, R. and Kalluri, H., 2019. Lung Cancer Detection Based on CT Scan Images by Using Deep Transfer Learning. Traitement du Signal, 36(4), pp.339-344.

[8] Masood, A., Sheng, B., Yang, P., Li, P., Li, H., Kim, J. and Feng, D.D., 2020. Automated decision support system for lung cancer detection and classification via enhanced RFCN with multilayer fusion RPN. IEEE Transactions on Industrial Informatics, 16(12), pp.7791-7801.

[9] Varchagall, M., Nethravathi, N.P., Chandramma, R., Nagashree, N. and Athreya, S.M., 2023. Using Deep Learning Techniques to Evaluate Lung Cancer Using CT Images. SN Computer Science, 4(2), p.173.

[10] Rahman, M.S., Shill, P.C. and Homayra, Z., 2019, February. A new method for lung nodule detection using deep neural networks for CT images. In 2019 International Conference on Electrical, Computer and Communication Engineering (ECCE) (pp. 1-6). IEEE.

[11] Raza, R., Zulfiqar, F., Khan, M.O., Arif, M., Alvi, A., Iftikhar, M.A. and Alam, T., 2023. Lung-EffNet: Lung cancer classification using EfficientNet from CT-scan images. Engineering Applications of Artificial Intelligence, 126, p.106902.

[12] Chenyang, L. and Chan, S.C., 2020. A joint detection and recognition approach to lung cancer diagnosis from CT images with label uncertainty. IEEE Access, 8, pp.228905-228921.

[13] Vaiyapuri, T., Liyakathunisa, Alaskar, H., Parvathi, R., Pattabiraman, V. and Hussain, A., 2022. Cat swarm optimization-based computer-aided diagnosis model for lung cancer classification in computed tomography images. Applied Sciences, 12(11), p.5491.
[14] Vishwa Kiran, S., Kaur, I., Thangaraj, K., Saveetha, V., Kingsy Grace, R. and Arulkumar, N., 2023. Machine Learning with Data Science-Enabled Lung Cancer Diagnosis and Classification Using Computed Tomography Images. International Journal of Image and Graphics, 23(03), p.2240002.
[15] Shankara, C. and Hariprasad, S.A., 2022. Artificial neural network for lung cancer detection using CT images. International Journal of Health Sciences, (II), pp.2708-2724.
[16] Gugulothu, V.K. and Balaji, S., 2023. A novel deep learning approach for the detection and classification of lung nodules from CT images. Multimedia Tools and Applications, pp.1-24.
[17] Nawreen, N., Hany, U. and Islam, T., 2021, July. Lung cancer detection and classification using CT scan image processing. In 2021 International Conference on Automation, Control and Mechatronics for Industry 4.0 (ACMI) (pp. 1-6). IEEE.
[18] Gugulothu, V.K. and Balaji, S., 2023. An early prediction and classification of lung nodule diagnosis on CT images based on hybrid deep learning techniques. Multimedia Tools and Applications, pp.1-21.
[19] Merlin Linda, G., Sree Rathna Lakshmi, N.V.S., Murugan, N.S., Mahapatra, R.P., Muthukumaran, V. and Sivaram, M., 2022. Intelligent recognition system for viewpoint variations on gait and speech using CNN-CapsNet. International Journal of Intelligent Computing and Cybernetics, 15(3), pp.363-382.
[20] Tsivgoulis, M., Papastergiou, T. and Megalooikonomou, V., 2022. An improved SqueezeNet model for the diagnosis of lung cancer in CT scans. Machine Learning with Applications, 10, p.100399.
[21] Reddy, A.S.K., Rao, K.B., Soora, N.R., Shailaja, K., Kumar, N.S., Sridharan, A. and Uthayakumar, J., 2023. Multi-modal fusion of deep transfer learning based COVID-19 diagnosis and classification using chest x-ray images. Multimedia Tools and Applications, 82(8), pp.12653-12677.
[22] Sasmal, B., Hussien, A.G., Das, A., Dhal, K.G. and Saha, R., 2023. Reptile Search Algorithm: Theory, Variants, Applications, and Performance Evaluation. Archives of Computational Methods in Engineering, pp.1-29.
[23] Wang, H., Luo, J., Zhu, G. and Li, Y., 2023. Enhanced Whale Optimization Algorithm with Wavelet Decomposition for Lithium Battery Health Estimation in Deep Extreme Learning Machines. Applied Sciences, 13(18), p.10079.
[24] http://www.via.cornell.edu/lungdb.html
[25] Yang, E., Shankar, K., Kumar, S., Seo, C., & Moon, I. (2023). Equilibrium Optimization Algorithm with Deep Learning Enabled Prostate Cancer Detection on MRI Images. Biomedicines, 11(12), 3200.
[26] Lakshmanaprabu, S.K., Mohanty, S.N., Shankar, K., Arunkumar, N. and Ramirez, G., 2019. Optimal deep learning model for classification of lung cancer on CT images. Future Generation Computer Systems, 92, pp.374-382.
[27] Vidyul Narayanan, Nithya P., Sathya M.. "Effective lung cancer detection using deep learning network." Journal of Cognitive Human-Computer Interaction, Vol. 5, No. 2, 2023 ,PP. 15-23 (Doi : https://doi.org/10.54216/JCHCI.050202)